Bull Volcanol (2008) 70:1103–1112
DOI 10.1007/s00445-007-0192-8

RESEARCH ARTICLE

Characterization of shape and terminal velocity of tephra particles erupted during the 2002 eruption of Etna volcano, Italy

M. Coltelli · L. Miraglia · S. Scollo

Received: 11 January 2007 / Accepted: 9 December 2007 / Published online: 27 March 2008

Abstract In this paper, we present a complete morphological characterization of the ash particles erupted on 18 December 2002 from Etna volcano, Italy. The work is based on the acquisition and processing of bidimensional digital images carried out by scanning electron microscopy (SEM) to obtain shape parameters by image analysis. We measure aspect ratio (AR), form factor (FF), compactness (CC), and rectangularity (RT) of 2065 ash particles with size between 0.026 and 1.122 mm. We evaluate the variation of these parameters as a function of the grain-size. Ash particles with a diameter of <0.125 mm vary from mostly equant to very equant, ash particles between 0.125 and 0.250 mm have an intermediate shape, and particles with diameters >0.250 mm are subelongate. We find that, on average, particles with a diameter of <0.250 mm are subrounded, particles between 0.250 and 0.50 mm are subangular, and particles >0.50 mm are angular. Using this morphological analysis and an empirical relation between the drag coefficient (C_D) and Reynolds number (R_e) of Wilson and Huang (Earth Planet Sci Lett 44:311–324, 1979), we calculate the terminal settling velocities (V_{WH}). The comparisons between these velocities and those calculated with the formula of Kunii and Levenspiel (*Fluidization engineering*. Wiley, New York, pp 97, 1969) (V_{KL}), which considers ash particles as spheres, show that V_{KL} are in average 1.28 greater than V_{WH}. Hence, we quantify the systematic error on the spatial distribution of the mass computed around the volcano carried out by tephra dispersal models when the particles are assumed to be spherical.

Keywords Mt. Etna · 2002 eruption · Scanning electron microscopy · Backscattered image analysis · Shape parameters · Terminal settling velocity · Tephra dispersal model

Editorial responsibility: J. C. Phillips

M. Coltelli · L. Miraglia · S. Scollo (✉)
Istituto Nazionale di Geofisica e Vulcanologia,
Sezione di Catania,
Piazza Roma 2,
95123 Catania, Italy
e-mail: scollo@ct.ingv.it

Introduction

Volcanic plume dynamics depends strongly on the interaction between the wind and the eruption column, forming strong or weak plumes when the rising velocity of the column is greater or smaller than the wind velocity (Sparks et al. 1997; Bonadonna and Phillips 2003). Sedimentation processes are mainly influenced by wind advection and terminal settling velocity of volcanic particles. Bonadonna et al. (1998) showed that particle settling behavior significantly affects the thinning rate of resulting tephra deposits. Hence, the accurate computation of terminal settling velocity is crucial to model the tephra deposits.

The terminal settling velocity of the volcanic particle is reached when the drag force, the aerodynamic force that opposes its motion through the air, is equal to the gravity force. It is given by:

$$V_T = \sqrt{\frac{4}{3}\frac{dg(\sigma-\rho)}{C_D\rho}} \quad (1)$$

where V_T is the terminal settling velocity of the particle (m s^{-1}), d is the particle diameter (m) that specifies the cross-sectional area of the particle, g is the gravitational acceleration (m s^{-2}), ρ and σ are the air and the particle

densities (kg m^{-3}), respectively, and C_D is the drag coefficient, which is a dimensionless parameter.

C_D depends on the particle shape and the Reynolds number (R_e) of the air flowing around it. R_e is a function of the viscous force that is caused by the friction acting on the particle surface and of the inertial force due to the air moving out of the particle's path, and is given as $R_e = \rho d V_T/\mu$ where μ is the air viscosity (Pa s).

C_D has been formulated on the basis of the experimental data available in the literature (Turton and Clark 1987; Haider and Levenspiel 1989; Swamee and Ojha 1991; Ganser 1993). Haider and Levenspiel (1989) presented a generalized expression for C_D:

$$C_D = \frac{24}{R_e}\left(1 + AR_e^B\right) + \frac{CR_e}{R_e + D} \quad (2)$$

where R_e is the Reynolds number, and A, B, C, and D are empirical constants calculated for eight different shapes from spheres to disks. For example, for a sphere they are A=0.1806, B=0.6459, C=0.4251, and D=6880.95 while for a disk oriented perpendicular to the flow direction they become A=2.5 B=0.21, C=15, and D=30.

Although it is well known that spherical and irregular particles experience different C_D, experimental data on V_T and C_D of irregular particles are still missing. In particular, there are only a few laboratory measurements aimed at evaluating the C_D of pyroclastic particles. Wilson and Huang (1979) reported experimental V_T for pumice, glass shards, and feldspar crystals with principal axial lengths between 59 and 1520 μm, finding that the terminal settling velocities measured were lower than those calculated, assuming particles as spheres. Based on laboratory data, they extrapolated the following law that describes the variation of C_D with the particle shape and R_e:

$$C_D = \frac{24}{R_e} \times F^{-0.828} + 2 \times \sqrt{1.07 - F} \quad (3)$$

where the parameter $F=(b+c)/2a$ is calculated using a, b, and c, which are the three principal axial lengths ($a>b>c$), and R_e is calculated from $d=(a+b+c)/3$. Terminal settling velocity is hence evaluated combining Eqs. 1 and 3.

Recently, Dellino et al. (2005) measured terminal settling velocity of pumice clasts from Vesuvio and Campi Flegrei, Italy using 3-D quantitative image analysis, and they found a new formula to predict V_T with an average error of 12%:

$$V_T = \frac{1.2065\mu\left(d^3 g(\sigma - \rho)\rho\Psi^{1.6}/\mu^2\right)^{0.5026}}{d\rho} \quad (4)$$

where μ is the air viscosity (Pa s) and Ψ is a shape factor, which is defined as the ratio of sphericity to circularity. The sphericity is the ratio between the surface areas of the equivalent sphere and the actual particle, whereas the circularity is the ratio between the particle perimeter and the perimeter of the circle equivalent to the maximum projected area.

The calculation of V_T by both formulae of Wilson and Huang (1979) and Dellino et al. (2005) requires detailed data on volcanic particle shapes. These data are often lacking and, therefore, in tephra dispersal models, the volcanic particles are assumed as spheres and V_T only depends on R_e (e.g., Heffter and Stunder 1993; Bonadonna et al. 2005; Searcy et al. 1998; Macedonio et al. 2005; Pfeiffer et al. 2005).

In this work, we measure the size and shape of ash particles erupted during the 2002 explosive activity of Etna volcano. We use 2-D backscattered SEM images, processing them with a standard image analysis to evaluate particle shapes (Miraglia 1996). The terminal settling velocity based on the formula of Wilson and Huang (1979), hereafter V_{WH}, is calculated using our particle shape data. Then, we apply the formula of Kunii and Levenspiel (1969), used also by Bonadonna et al. (1998), to calculate the settling velocity, hereafter V_{KL}, assuming ash particles to be spheres:

$$V_T = (3.1 g\sigma d/\rho)^{1/2} (R_e > 500) \quad (5)$$

$$V_T = \left(g\sigma d^2/18\mu\right) (R_e < 0.4) \quad (6)$$

$$V_T = d\left(4\sigma^2 g^2/225\mu\rho\right)^{1/3} (0.4 < R_e < 500) \quad (7)$$

Finally, we compare the results between V_{WH} and V_{KL} and then we evaluate the differences in the mass distribution computed by a tephra dispersal model due to the different terminal settling velocities.

The 2002–2003 eruption

The 2002–2003 eruption began in the evening of 26 October 2002 and ended on 28 January 2003 after almost 3 months of continuous explosive and effusive activity (Andronico et al. 2005). The eruptive activity involved the S flank of the volcano where a NS, 1-km-long fissure opened between 2850 and 2600 m and the NE flank where a 3.7-km-long fissure opened from 2500 to 1890 m (Andronico et al. 2005). Violent strombolian activity, fire fountaining, and effusive activity occurred from both the fissures up to 5 November after the activity occurred only at the S fissure. Fire fountains from that vent formed a long-lasting eruption column until the end of December. The maximum column height reached 7 km a.s.l. Because of the wind, prevailing lapilli and ash covered mainly the south and east volcano sectors. Fine ashes

reached the Aeolian Islands, central Italy, western Greece, and Libya, as far as 500 km from the volcano. The erupted pyroclastic total volume was estimated by Andronico et al. (2005) between 40 and 50×10^6 m^3. The singular explosive activity makes the 2002–2003 eruption a unique event in the last 300 years, comparable only with La Montagnola eruption that occurred in 1763 (Branca and Del Carlo 2005; Sturiale 1970) and the 21–24 July explosive phase of the 2001 eruption (Scollo et al. 2007).

Volcanic ash analyzed in this paper was collected on 18 December 2002 at Piano del Vescovo about 5 km from the volcanic vent (Scollo et al. 2005). During that day, the intensity of the eruption remained at medium–high levels producing the eruptive column about 4000 m a.s.l., and the volcanic clouds flowed forward S–SE.

Morphological characterization

We measured 2065 ash particles, between 0.026 and 1.122 mm, collected on 18 December 2002 at Piano del Vescovo (Fig. 1) along the dispersion axes of the ash plume. Ash particles were mainly composed of slightly vesicular juvenile clasts, tachylite, and sideromelane that showed irregular shapes and a smaller amount of lithics and minerals having smooth edges. Ash particles were divided into six Φ classes using a set of sieves with mesh sizes spaced at one Φ ($\Phi=-\log_2(d)$ where d is the particle diameter in mm), and arranged on six microscope mounts of 8 cm^2, avoiding any touching or partial overlapping (Fig. 2). Each mount was carbon coated and analyzed using a SEM LEO 1430 linked to an INCAENERGY Spectrometer, at the Catania Section of INGV. Thirty-four bidimensional images were selected to include all the particles and analyzed by using the NIH IMAGE public-domain software. Ash particles were automatically recognized using dedicated thresholds and then some nondimensional parameters were calculated to evaluate the shape characteristics (Russ 1995; Dellino and La Volpe 1996; Riley et al. 2003).

We measured breadth and width, defined respectively as the length of the major and minor axes of the ellipse that best fit the particle, area as the sum of the pixels of the particles including the pores, and perimeter as the length around the outside of the particle boundary. Hence, we calculated: aspect ratio (AR), defined as width/breadth that reflects only the overall elongation of particles but does not make a distinction between squares and circles; form factor (FF), as 4πarea/perimeter^2 describing the surface irregularities or roughness (Russ 1995); compactness (CC), as area/(breadth×width); and rectangularity (RT), as perimeter/(2breadth+2width). These parameters are considered by Dellino and La Volpe (1996) as a set of 'robust' shape descriptors.

For all ash particles, we calculated the mean, standard deviation (SD), and the mode of AR, FF, CC, and RT. The results are reported in Table 1 and plotted in Fig. 3, except the CC values because it showed a narrow range between 0.78 and 0.81, which indicates that the particles are more similar to circles than rectangles.

AR values range between 0.2 and 1 and seem to be independent of the grain-size class even though the mode changes with size (Fig. 3 and Table 1). On the basis of the Folk (1974) scheme, ash particles can be classified as very elongate (AR<0.6), elongate (0.6<AR<0.63), subelongate (0.63<AR<0.66), intermediate shape (0.66<AR<0.69),

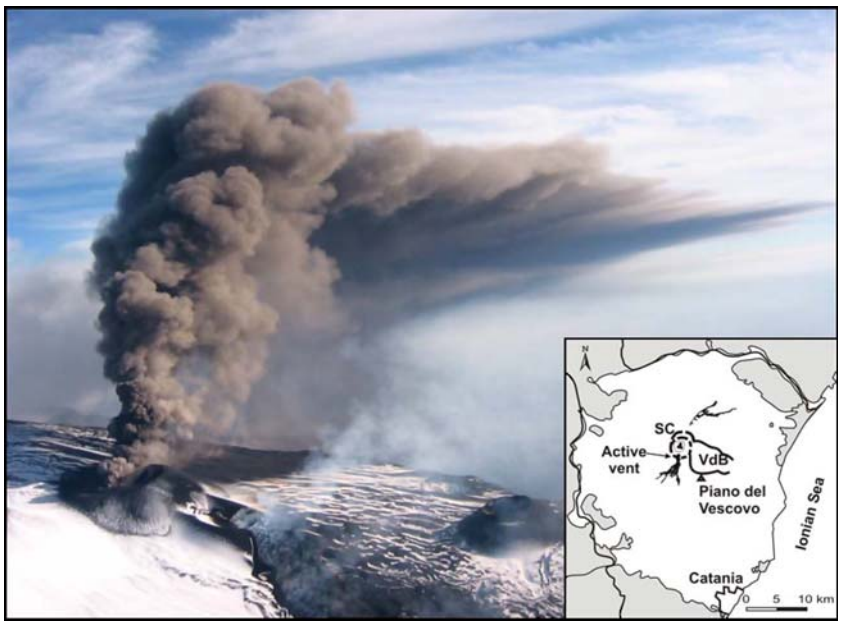

Fig. 1 Volcanic plume formed during the 2002–2003 Etna eruption. The picture was taken during the monitoring activities of INGV in Catania. In the *right lower corner*, a sketch map of Etna volcano: the sedimentary basement is in *gray*, the volcanic rocks are in *white*, and the 2002–2003 lava flows formed from the NE and S eruptive fissures are in *black*. *SC* summit craters, *VdB* Valle del Bove. The *black triangle* indicates the sampling site (Piano del Vescovo)

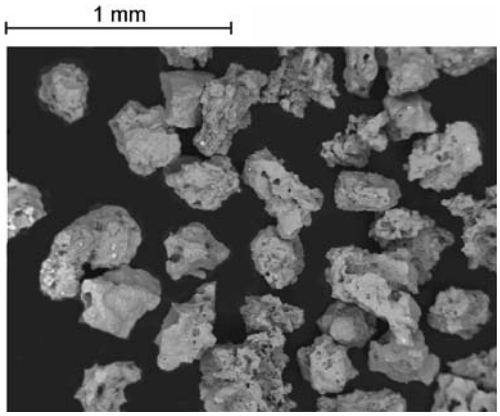

Fig. 2 Backscattered images of ash particles erupted on 18 December 2002 from the Etna volcano. Ash particles were arranged on apposite microscope mounts (8 cm^2). They showed blocky shape and irregular contours

subequant (0.69<AR<0.72), equant (0.72<AR<0.75), and very equant (AR>0.75). The percentage distribution of all particles analyzed is 21.8% of very elongate particles, 6.8% of elongate, 7.3% of subelongate, 8% of particles having intermediate shape, 7.4% of subequant particles, 8.4% of equant, and 40.3% of very equant particles.

While there are no significant differences of the mean value of AR between each grain-size, the mode decreases with the particle size. In fact, the particles belonging to Φ=0 and Φ=1 classes have the mode peak on subelongate particles, the particles belonging to Φ=2 have mainly an intermediate shape, equant are mainly particles of Φ=3 class, and very equant are particles belonging to Φ=4 class. Furthermore, the AR values >0.72 belong mainly (about 80% of particles) to Φ=4 grain-size class (diameter<0.063 mm). This evidence suggests that the smallest particles result from larger particles breaking on contact with the ground.

FF ranges widely from 0.26 to 1. In particular, particles belonging to Φ=0 and Φ=1 have lower values of FF than smaller size classes with a mode of 0.64 and 0.62, respectively, whereas the particles of smaller size (Φ=2, Φ=3, and Φ=4) have a higher mode (i.e., 0.7, 0.76, and 0.68, respectively; Fig. 3 and Table 1). RT values are instead always >0.8 and show again two important variations between the grain-size classes. In fact, particles belonging to Φ=0 and Φ=1 have both the mode equal to 1, while particles belonging to Φ=2, Φ=3, and Φ=4 have lower values, being 0.92, 0.9, and 0.88, respectively.

FF and RT allow us to discriminate particles on the basis of surface irregularities (Dellino and La Volpe 1996). Therefore, we calculated the FF and RT of particles belonging to the comparative chart of Russel, Taylor, and Pettijohn (in Muller 1967) that are arranged in five classes of roundness from angular to well-rounded (Table 2 and Fig. 4). Hence, Etna ash particles were compared and classified using the FF and RT in the same classes of roundness of the comparative chart.

Results show that ash particles collected are mainly subangular. On average, particles belonging to Φ=0 classes are angular, particles of Φ=1 class are subangular, and particles belonging to Φ=2, Φ=3 and Φ=4 classes are subrounded (Fig. 5 and Table 1).

Terminal settling velocity

Terminal settling velocity was calculated using the formula of Wilson and Huang (1979) for which the particles were assumed to be prolate spheroids (where $a>b=c$). Terminal settling velocity was also calculated for comparison with the formula of Kunii and Levenspiel (1969) that instead approximates particles as spheres with diameter equal to $(a+b+c)/3$ where b=c. We found that V_{WH} is on average lower than V_{KL} by up to 47.9% (Fig. 6).

Recently, Riley et al. (2003) measured the shape, size, and terminal settling velocity of the ash particles having dimensions between 10 and 150 μm collected in three distal fallout deposits. Their measurements showed that ash particles differed greatly from a sphere, and their diameters were much greater (between 10% and 120%) than the ones

Table 1 Mean, SD, Mode of AR, FF, CC, RT, and the number (*N*) of Etna ash particles analyzed

	Mean	SD	Mode	*N*
AR				
$\Phi\geq0$	0.704	0.308	0.66	2065
Φ=0	0.709	0.293	0.63/0.72	253
Φ=1	0.735	0.410	0.63	190
Φ=2	0.673	0.302	0.66	817
Φ=3	0.720	0.291	0.72	742
Φ=4	0.793	0.221	0.75	63
FF				
$\Phi\geq0$	0.660	0.108	0.68	2065
Φ=0	0.605	0.186	0.64	253
Φ=1	0.617	0.197	0.62	190
Φ=2	0.688	0.172	0.70	817
Φ=3	0.729	0.155	0.76	742
Φ=4	0.723	0.158	0.68	63
CC				
$\Phi\geq0$	0.785	0.003	0.786	2065
Φ=0	0.785	0.002	0.785	253
Φ=1	0.785	0.0004	0.886	190
Φ=2	0.785	0.001	0.787	817
Φ=3	0.785	0.005	0.790	742
Φ=4	0.785	0.010	0.789	63
RT				
$\Phi\geq0$	0.934	0.104	0.92	2065
Φ=0	0.991	0.142	1.00	253
Φ=1	0.974	0.122	1.00	190
Φ=2	0.933	0.086	0.92	817
Φ=3	0.917	0.054	0.90	742
Φ=4	0.927	0.106	0.88	63

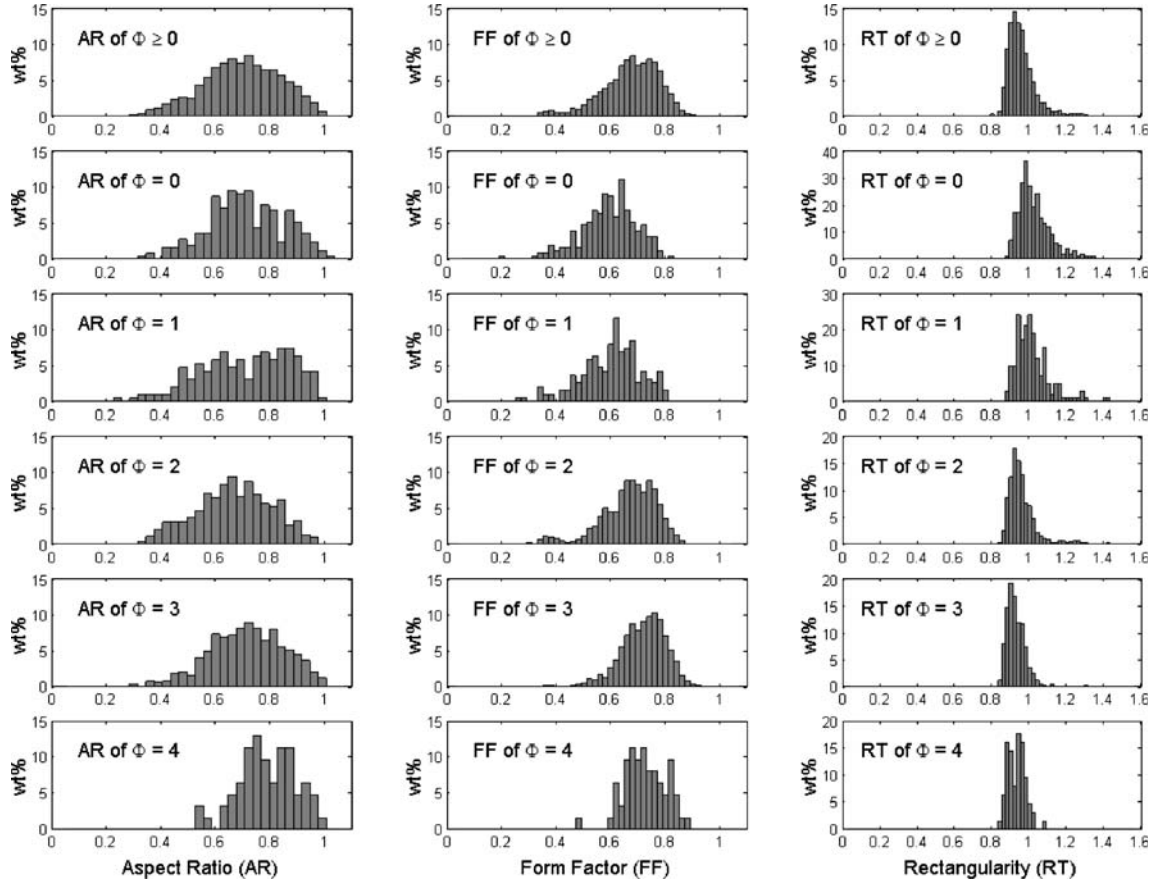

Fig. 3 Frequency distribution of the AR, FF, and RT values calculated for different grain-size classes

predicted for spherical particles with the same terminal settling velocities. This means that the terminal settling velocity greatly diminishes with the irregular shape. Likewise, we compared the diameter of each ash particle with the diameter of the spherical particle that should fall at the same V_{WH} velocity, calculated by following the formula of Kunii and Levenspiel (1969). We found that the diameters of the ash particles measured were larger from 7% to 66% than the diameters of spheres (Fig. 7), which in agreement with the results obtained by Riley et al. (2003).

Grouping all particles in AR classes of 0.1, we calculate the mean ratio and the corresponding SD of V_{WH}/V_{KL}. Figure 8 shows a linear relation between V_{WH}/V_{KL} and AR shape parameter, and in the AR ranges between 0.3 and 0.9, we can state this relationship as:

$$\frac{V_{WH}}{V_{KL}} = (0.6 \times AR + 0.4) \quad (8)$$

Through this type of image analysis applied to the volcanic particles, V_{WH} could be easily calculated from the AR values. Nevertheless, we emphasize that this relation is not representative of all volcanic particles but that formula is representative only for the type of eruption analyzed. Other shape investigation of particles ejected during eruptions with different styles should be performed.

Table 2 FF and RT of particles belonging to the comparative chart (Muller 1967). This is used to classify Etna ash particles following the same class of roundness.

	FF	RT	FF	RT	FF	RT	FF	RT	FF	RT
Angular	0.608	1.008	0.579	0.988	0.535	1.142	0.436	1.154	0.526	0.964
Subangular	0.636	0.942	0.643	0.937	0.658	0.938	0.608	0.984	0.636	0.955
Subrounded	0.665	0.921	0.724	0.897	0.713	0.893	0.663	0.933	0.694	0.886
Rounded	0.739	0.872	0.734	0.858	0.732	0.877	0.736	0.876	0.754	0.876
Well-rounded	0.860	0.830	0.792	0.812	0.770	0.811	0.847	0.826	0.841	0.827

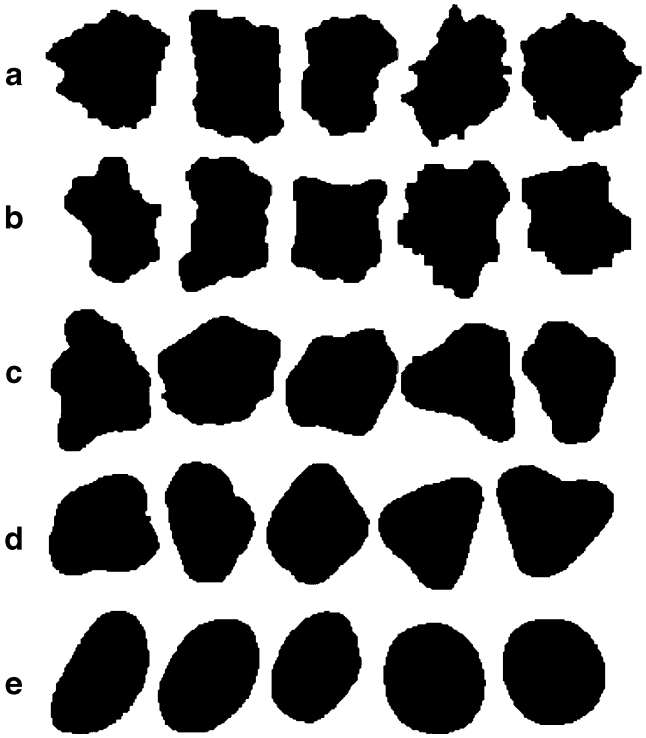

Fig. 4 Comparative chart of Russel, Taylor, and Pettijohn (in Muller 1967). **a** Angular clasts, **b** subangular clasts, **c** subrounded clasts, **d** rounded clasts, and **e** well-rounded clasts

Terminal velocities are lower when calculated with the formula of Wilson and Huang (1979) than those calculated with the formula of Kunii and Levenspiel (1969) (Fig. 9). In fact, from our data, we found that the 23.3% of the V_{KL} velocities have values <0.4 m s^{-1} while the V_{KL} are 37.7%. The effect of shape on terminal settling velocity is crucial.

Finally, we evaluated the effect on the total mass distribution computed by a tephra dispersal model when V_{WH} and V_{KL} are used as input data in two different simulations. For the test, we used the HAZMAP model

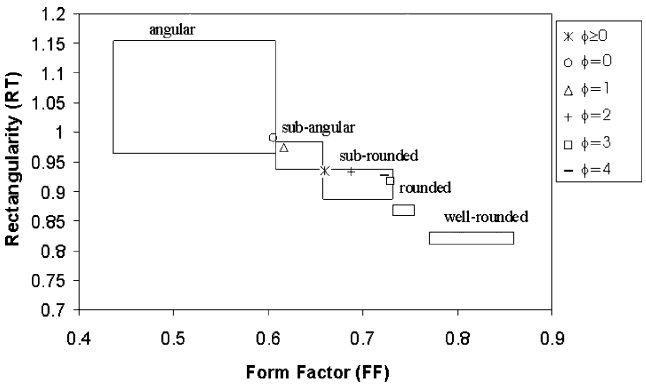

Fig. 5 FF vs RT plot of the values obtained by the morphological analysis of the Etna particles (Table 1). The regions identified as angular, subangular, subrounded, rounded, and well-rounded were obtained from the comparative chart of Russel, Taylor, and Pettijohn (in Muller 1967; Table 2)

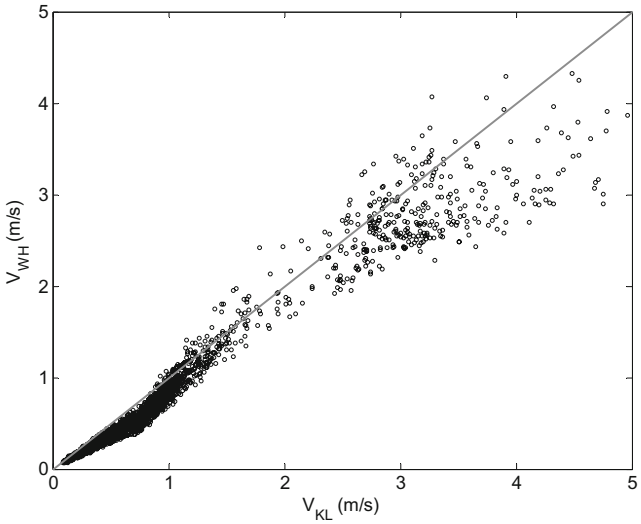

Fig. 6 Comparisons between terminal settling velocities V_{KL} (calculated by the formula of Kunii and Levenspiel 1969), approximating ash particles to spheres, and terminal settling velocities V_{WH} (calculated by the formula of Wilson and Huang, 1979) for which particle shape is considered. Perfect agreement is indicated by the *gray line*. Ash particle density is equal to 1.84±0.38 g cm^{-3}, obtained from density measurements of 20 particles by the hydrostatic balance

(Macedonio et al. 2005) where the terminal settling velocity distribution is divided into 15 classes derived from the total grain-size distribution. As the input parameter, we chose an eruption column of 4.5 km (a.s.l) that was the mean value of the column height during the 2002 Etna eruption and a constant direction and speed of wind blowing toward the east. Hence, we computed the mass fallen around the volcano. Because the irregular particle shape reduces terminal settling velocities, there is an increase of the total

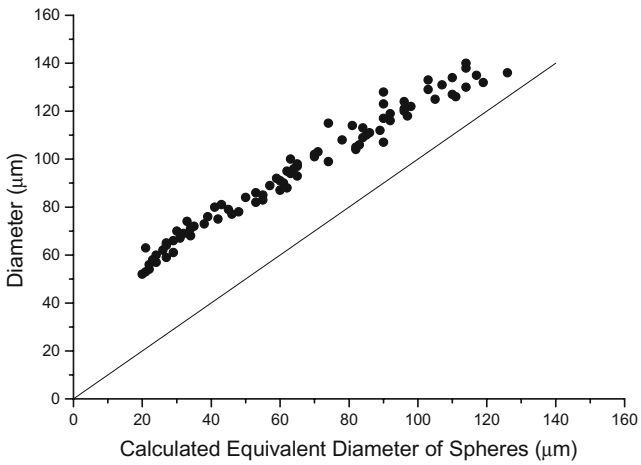

Fig. 7 Diameter of ash particles (given by $d=(a+b+c)/3$) compared to diameters of spheres falling at the same terminal settling velocities of ash particles. The terminal settling velocities of ash particles were calculated by using the formula of Wilson and Huang (1979) while the calculated diameters of the spheres were computed inverting the formula of Kunii and Levenspiel (1969)

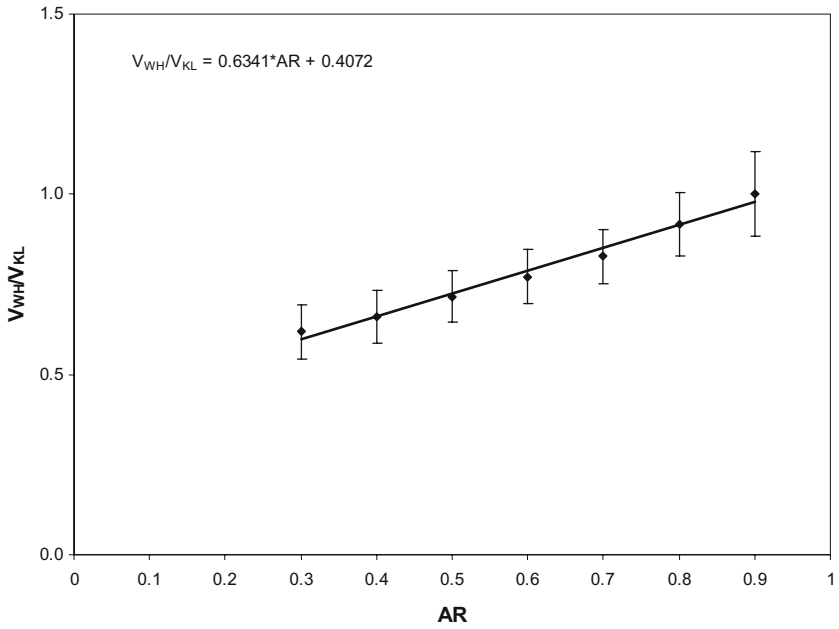

Fig. 8 Linear relation between the mean values of the ratio V_{WH}/V_{KL} and the shape parameter AR of ash particles grouping in 0.1. The *error bar* is the corresponding SD

mass computed by the model that uses V_{WH} in the medial and distal region from the vent. In the absence of wind, this marker happens at about 2.5 km from the vent. In the presence of wind, it is shifted toward the wind direction: about 3.5 km for a wind speed of 5 m s^{-1}, 4.5 km for a wind speed of 10 m s^{-1}, and 6.5 km for a wind speed of 20 m s^{-1} (Fig. 10). In the absence of wind, the total mass computed using the two terminal settling formulae differs by 20% at 10 km, 70% at about 20 km, and 90% at about 25 km from the vent. In the presence of a wind speed of 20 m s^{-1}, the differences between the two computed masses are located at about 28, 37, and 43 km far from the vent.

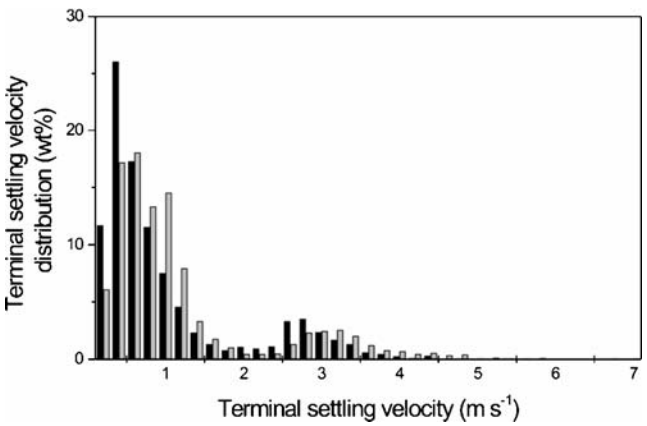

Fig. 9 Comparison between the terminal settling velocity V_{WH} (*black bars*) distribution, calculated by the formula of Wilson and Huang (1979), and the terminal settling velocity V_{KL} (*gray bars*) distribution, calculated by the formula of Kunii and Levenspiel (1969). The V_{WH} distribution has a greater percentage of particles with lower velocity than V_{KL}

Discussion

During the 2002–2003 Etna eruption, a new instrument, originally designed as a rain gauge disdrometer, was used to investigate the terminal settling velocity of volcanic particles (Scollo et al. 2005). The instrument is an X-band continuous wave radar and is based on the Doppler shift induced by falling particles on the transmitted electromagnetic wave (Prodi et al. 2000). The radar detected the terminal settling velocities of the falling particles (Scollo et al. 2005), and their values were in the same range as those measured experimentally (Wilson and Huang 1979) and calculated analytically (Kunii and Levenspiel 1969) for spherical particles with similar dimension and density. Nevertheless, during the two field tests, only four distinct velocity peaks were observed that could be related to aggregation into preferential aerodynamic diameters or caused by settling-driven instabilities (Scollo et al. 2005). The same particles were hence analyzed in this paper to investigate the effects of the particle shape on terminal settling velocity. We found that the terminal settling velocity distribution V_{WH} calculated by the formula of Wilson and Huang (1979) has a greater percentage of particles with lower velocity than V_{KL}, calculated by the formula of Kunii and Levenspiel (1969). Nevertheless, the terminal settling velocity distribution V_{KL}, calculated including the particle shape, presents a continuous spectrum that differs from the four peaks found during the 2002 field test. Even in this case, the measured velocities fall inside the velocity distribution V_{WH}. However, the analysis has shown that the particles measured from disdrometer have very irregular shape. Huber and Sommerfeld (1994) found

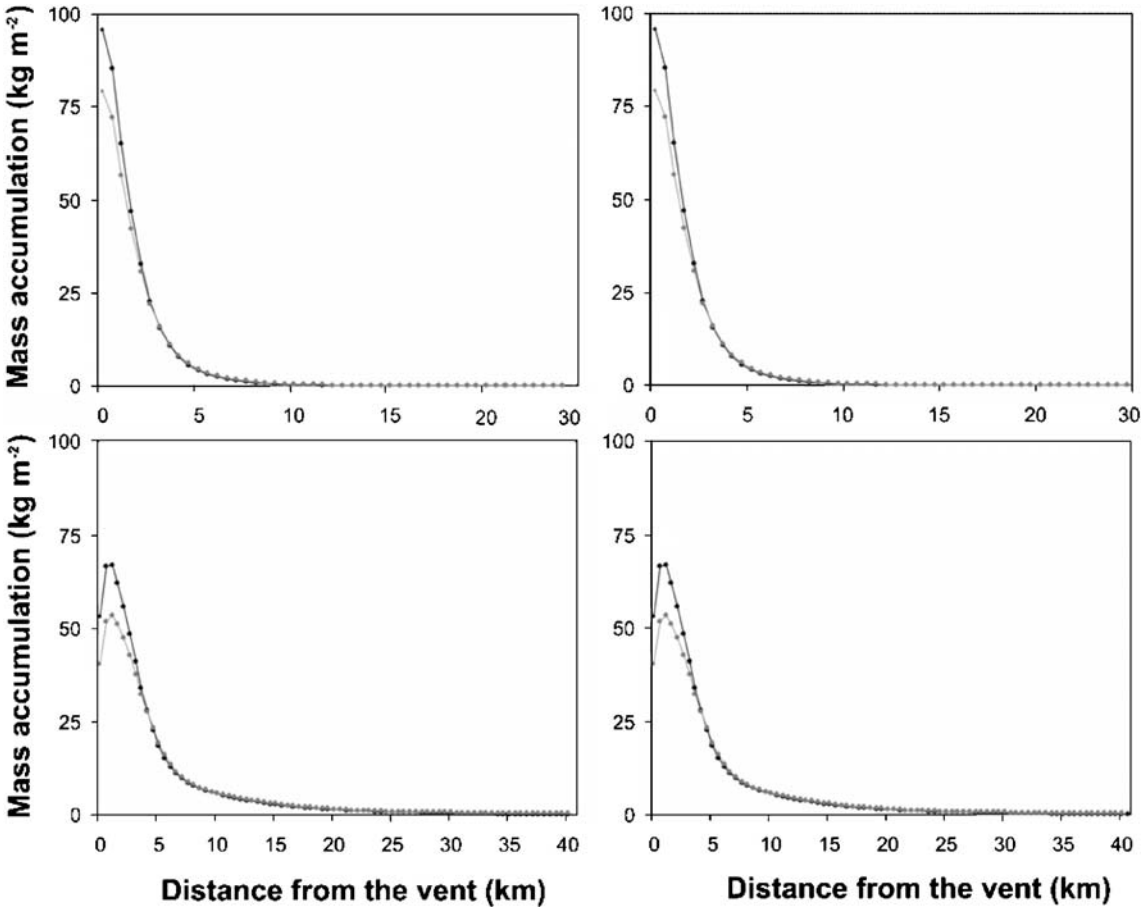

Fig. 10 Mass accumulation (kg m^{-2}) along the wind direction computed considering an eruption with similar features of 2002 Etna eruption and four different wind speeds: 0, 5, 10, and 20 m s^{-1}. Mass accumulation in *black* is calculated using the formula of Kunii and Levenspiel (1969) while mass accumulation in *gray* is calculated using the formula of Wilson and Huang (1979) in which the particle shape is considered

that dispersed two-phase air and particle flows in a pipe show inhomogeneous shape in both transverse and streamwise directions. Because irregular particles with the same density and size range can produce quite different velocity profiles, this effect could occur during the sedimentation process in air and could be demonstrated only considering more complex phenomena such as particle interactions or electrostatic phenomena (Holasek and Self 1995; Gilbert and Lane 1994).

A first semiquantitative shape characterization of Etna particles was carried out during the 2001 explosive eruption by Taddeucci et al. (2002) that found particle shapes covering a wide range from rounded to irregular. Instead, we made a more quantitative shape characterization through the image analysis of 2065 particles suitable for the further statistical analysis. The quantitative shape characterization furnished by the AR and FF parameters could be easily automated in the particle analysis during the Etna explosive eruptions. The analysis should be carried out considering all the particle sizes together because we noted that shape parameters were only weakly dependent on size.

The analysis of the particle shape showed that their approximation as spheres is reasonable for calculating settling velocities only for the particles belonging to the class $\Phi=4$ corresponding to the smaller size. In fact, only these are both very equant ($0.75<AR<1$) and also subrounded (see FF and RT on Table 1 and Fig. 3). This is also in agreement with classic theory, which shows that the C_D of particles in the laminar regimes ($R_e<0.4$) is not significantly affected by the particle shape. Nevertheless, tephra deposits are formed by particles belonging to intermediate and high Reynolds regime (Bonadonna et al. 1998) where the approximation to a sphere is, hence, not realistic. Furthermore, in our samples, perfectly equant clasts ($AR=1$) are present only in a small percentage (<1%) confirming that the simple approximation of ash particle is not correct.

The main problem is that few data on settling velocities of natural clasts are available (Walker 1971; Wilson and Huang 1979; Lane et al. 1993) and because the shapes are irregular and the density is inhomogeneous, the terminal settling velocity must be determined empirically (Bursik 1998).

Tephra dispersal models usually apply algorithms of terminal settling velocity that approximate ash particles as spheres. Therefore, this approximation introduces a systematic error in the evaluation of the mass distribution computed by models. In fact, it is well known that the terminal settling velocity has a first-order effect on the results of tephra dispersal models (Pfeiffer et al. 2005) and strongly influences the sedimentation processes of the volcanic clouds (Bonadonna et al. 1998). Our results showed that the distribution of the total mass calculated by the tephra dispersal models differs by values ranging from 20% to 90% when the two velocity sets are used as input data. Some tephra dispersal models already account for a parameterization of the effect of particle shape on terminal velocity (e.g., Suzuki 1983, Armienti 1988). However, given that these parameterizations are often based on particle measurements that are difficult to make, they are also often neglected. Equation 8 presented in this manuscript could largely simplify the calculation of the terminal velocity for irregular particles. However, more work needs to be done and more particles need to be investigated to make this equation more general and statistically representative.

Furthermore, Riley et al. (2003) demonstrated that the AR is the more distinctive parameter in the valuation of terminal settling velocity. They found that basaltic particles are more rounded than the silicic particles, and fixed a value of the AR (defined in their work as breadth/width) equal to 1.5 for andesitic and basaltic ashes, and from 1.5 to 2.6 for the rhyolitic ashes. Using the same definition, we calculated a mean value (on all 2065 particles) equal to 1.55. This confirms that the results obtained from Riley et al. (2003) are correct for a basaltic volcano like Etna and this value could be used to include the particle shape in the tephra dispersal models as a first approximation.

Concluding remarks

Through the first fully quantitative analysis of ash shape produced during a basaltic explosive eruption of Etna, we demonstrate that the ash collected had irregular shapes, varying from very equant to elongate and from rounded to angular. Through image analysis, we calculated the shape parameters that have been used to evaluate V_{WH}, resulting lower than V_{KL} ones and their ratio follows a linear relation with AR.

In the future, increasing our knowledge of the relation between the terminal settling velocity of volcanic particles and their irregular shape, other parameterizations could be used to include the effect of other shape parameters, e.g., FF and RT, which are easy to measure like AR. In this way, the approach of Dellino et al. (2005) that uses both quantitative shape analysis and experimental data of terminal settling velocity, seem promising.

Finally, tephra dispersal models should include the shape parameter of ash particles as input data to aim at further reducing the differences between tephra deposits computed by numerical models and those really produced during explosive eruptions.

Acknowledgements The authors are grateful to G. Bluth, A. Costa and P. Dellino for the useful discussions on particle shape analysis. We greatly thank the two reviewers C. Bonadonna and L. Mastin, and the associate editor J. Phillips for their valuable suggestions that improved the quality of the paper. This research was supported by an INGV-GNV fellowship and then by the FIRB Italian project "Sviluppo Nuove Tecnologie per la Protezione e Difesa del Territorio dai Rischi Naturali" funded by Italian Minister of University and Research (S. Scollo).

References

Andronico D, Branca S, Calvari S, Burton MR, Caltabiano T, Corsaro RA, Del Carlo P, Garfì G, Lodato L, Miraglia L, Muré F, Neri M, Pecora E, Pompilio M, Salerno G, Spampinato L (2005) A multi-disciplinary study of the 2002–03 Etna eruption: insights for a complex plumbing system. Bull Volcanol 67 (4):314–330 DOI 10.1007/s00445-004-0372-8

Armienti P, Macedonio G, Pareschi MT (1988) A numerical-model for simulation of tephra transport and deposition—applications to May 18, 1980, Mount-St-Helens eruption. J Geophys Res 93:6463–6476

Bonadonna C, Ernst GGJ, Sparks RSJ (1998) Thickness variations and volume estimates of tephra fall deposits: the importance of particle Reynolds number. J Volcanol Geotherm Res 81:173–187

Bonadonna C, Phillips JC (2003) Sedimentation from strong volcanic plumes. J Geophys Res 108(B7), Art. No. 2340. DOI 10.1029/2002JB002034

Bonadonna C, Connor CB, Houghton BF, Sahetapy-Engel S, Hincks T, Connor L (2005) Probabilistic modeling of tephra dispersion: Hazard assessment of a multi-phase rhyolitic eruption at Tarawera, New Zealand. J Geophys Res 110(B3), Art. No. B03203. DOI 10.1029/2003JB002896

Branca S, Del Carlo P (2005) Types of eruptions of Etna volcano AD 1670–2003: implications for short-term eruptive behaviour. Bull Volcanol 67(8):732–742

Bursik M (1998) Tephra dispersal. In: Gilbert JS, Sparks RSJ (eds) The physics of explosive volcanic eruptions. Geological Society, London, pp 115–144

Dellino P, La Volpe L (1996) Image processing analysis in reconstructing fragmentation and transportation mechanisms of pyroclatic deposits. The case of Monte Pilato-Rocche Rosse eruptions, Lipari (Aeolian Islands, Italy). J Volcanol Geotherm Res 71:13–29

Dellino P, Mele D, Bonaria R, Braia G, La Volpe L, Sulpizio R (2005) The analysis of the influence of pumice shape on its terminal velocity. Geophys Res Lett 32, Art. No. L21306. DOI 10.1029/2005GL023954

Folk RL (1974) Petrology sedimentary rocks. Hemphill, Austin, Texas, p 182

Ganser H (1993) A rational approach to drag prediction of spherical and non spherical particles. Powder Technol 77:143–152

Gilbert JS, Lane SJ (1994) The origin of accretionary lapilli. Bull Volcanol 56:398–411

Haider A, Levenspiel O (1989) Drag coefficient and terminal velocity of spherical and non spherical particles. Powder Technol 58:63–70

Heffter JL, Stunder BJB (1993) Volcanic ash forecast transport and dispersion (Vaftad) model. Weather Forecast 8:533–541

Holasek RE, Self S (1995) GOES weather satellite observations and measurements of the may 18, 1980, Mt. St. Helens, 1995. J Geophys Res 100:8469–8487

Huber N, Sommerfeld M (1994) Characterisation of the cross-sectional particle concentration distribution in pneumatic conveying systems. Powder Technol 79:191–210

Kunii DK, Levenspiel O (1969) Fluidization engineering. Wiley, New York, p 97

Lane SJ, Gilbert JS, Hilton M (1993) The aerodynamic behaviour of volcanic aggregates. Bull Volcanol 55:481–488

Macedonio G, Costa A, Longo V (2005) A computer model for volcanic ash fallout and assessment of subsequent hazard. Comput Geosci 31:837–845

Miraglia L (1996) Indagini petrografiche quantitative su vulcanite etnee: Confronto tra metodologie tradizionali e computer-assistite. M.S. thesis, University of Catania, Italy, pp 80

Muller G (1967) Methods in sedimentary petrology. Hafner, New York

Pfeiffer T, Costa A, Macedonio G (2005) A model for the numerical simulation of tephra fall deposits. J Volcanol Geotherm Res 140:273–294

Prodi F, Tagliavini A, Medini R (2000) Time variability in rainfall events observed by Pludix. Phys Chem Earth, Part B Hydrol Oceans Atmos 25:959–963

Riley CM, Rose WI, Bluth GJS (2003) Quantitative shape measurements of distal volcanic ash. J Geophys Res 108(B10), Art. No. 2504. DOI 10.1029/2001JB000818

Russ J (1995) The image processing handbook, 2nd edn. CRC, Boca Raton, FL, p 674

Searcy C, Dean K, Stringer W (1998) PUFF: A high resolution volcanic ash tracking model. J Volcanol Geotherm Res 80:1–16

Scollo S, Coltelli M, Prodi F, Folegani S, Natali S (2005) Terminal settling velocity measurements of volcanic ash during the 2002–2003 Etna eruption by an X-band microwave rain gauge disdrometer. Geophys Res Lett 32, Art. No. L10302. DOI 10.1029/2004GL022100

Scollo S, Del Carlo P, Coltelli M (2007) Tephra fallout of 2001 Etna flank eruption: analysis of the deposit and plume dispersion. J Volcanol Geoth Res 160:147–164

Sparks RSJ, Bursik MI, Carey SN, Gilbert JS, Glaze LS, Sigurdsson H, Woods AW (1997) Volcanic plumes. Wiley, Chichester

Sturiale C (1970) La singolare eruzione dell'Etna del 1763 "La Montagnola". Rend Soc Ital Mineral Petrol 26:314–351

Suzuki T (1983) A theoretical model for dispersion of tephra. In: Shimozuru D, Yokoyama I (eds) Arc volcanism, physics and tectonics. Terra Scientific Publishing Company (TERRAPUB), Tokyo, pp 95–113

Swamee PK, Ojha CSP (1991) Drag coefficient and fall velocity of non-spherical particles. J Hydraul Eng 117:660–667

Taddeucci J, Pompilio M, Scarlato P (2002) Monitoring the explosive activity of the July–August 2001 eruption of M. Etna (Italy) by ash characterization. Geophys Res Lett 29, Art. No. 1230. DOI 10.1029/2001GL014372

Turton R, Clark NN (1987) An explicit relationship to predict spherical particle terminal velocity. Powder Technol 53:127–129

Walker GPL (1971) Grain-size characteristics of pyroclastic deposits. J Geol 79:696–714

Wilson L, Huang TC (1979) The influence of shape on the atmospheric settling velocity of volcanic ash particles. Earth Planet Sci Lett 44:311–324